

Comparative Analysis of Human Embryonic Stem Cell and Induced Pluripotent Stem Cell-Derived Hepatocyte-Like Cells Reveals Current Drawbacks and Possible Strategies for Improved Differentiation

Justyna Jozefczuk,¹ Alessandro Prigione,¹ Lukas Chavez,¹ and James Adjaye^{1,2}

Hepatocytes derived from human embryonic stem cells (hESCs) or induced pluripotent stem cells (iPSCs) could provide a defined and renewable source of human cells relevant for cell replacement therapies and toxicology studies. However, before patient-specific iPSCs can be routinely used for these purposes, there is a dire need to critically compare these cells to the golden standard—hESCs. In this study, we aimed at investigating the differences and similarities at the transcriptional level between hepatocyte-like cells (HLCs) derived from both hESCs and iPSCs. Two independent protocols for deriving HLCs from hESCs and iPSCs were adopted and further characterization included immunocytochemistry, real-time (RT)-polymerase chain reaction, and in vitro functional assays. Comparative microarray-based gene expression profiling was conducted on these cells and compared to the transcriptomes of human fetal liver and adult liver progenitors. HLCs derived from hESCs and human iPSCs showed significant functional similarities, similar expression of genes important for liver physiology and common pathways. However, specific differences between the 2 cell types could be observed. For example, among the cytochrome P450 gene family, *CYP19A1*, *CYP1A1*, and *CYP11A1* were enriched in hESC-derived HLCs, and *CYP46A1* and *CYP26A1* in iPSC-derived HLCs. HLCs derived from hESCs and human iPSCs exhibited broad similarities but as well meaningful differences. We identified common upregulated transcription factors, which might serve as a source for generating a cocktail of factors able to directly transdifferentiate somatic cells into HLCs. The findings may be vital to the refinement of protocols for the efficient derivation of functional patient-specific HLCs for regenerative and toxicology studies.

Introduction

CURRENTLY, CHRONIC LIVER DISEASES can only be treated effectively applying transplantation surgery. This treatment is very limited due to the dependence on the availability of donated organs. An alternative therapeutic approach would be to increase the number of functional hepatocytes by cell transplantation. Especially since the potential of cell replacement therapy has already been demonstrated by the use of primary adult hepatocytes in animal models of liver diseases [1]. In addition, the primary human hepatocytes (PHHs) routinely applied in drug toxicology assays possess several constraints, including heterogeneity and limited culture potential. Differentiation protocols triggering cultured pluripotent human embryonic stem cells (hESCs) into functional hepatocytes have been found to mimic hepatogenesis by addition of soluble medium factors and reconstruction of cell-matrix [2–5]. These derived hepatocytes could thus provide a

defined and renewable source of human cells relevant for cell therapies and also for industrial in vitro tests.

Recently, the generation of hepatocyte-like cells (HLCs) has been also demonstrated to be feasible with human-induced pluripotent stem cells (iPSCs) [6–9], which are a novel stem cell type derived from somatic cells through ectopic expression of a defined set of transcription factors normally expressed in ESCs [10–13]. Indeed given their isogenic nature, iPSCs appear as a promising source for patient-specific hepatocytes [14–16]. However, recent genome-wide analysis revealed specific gene expression differences between hESCs and iPSCs [17]. Moreover, distinct differentiation potential and functional differences between iPSC and ESC derivatives have been demonstrated [18].

In an attempt to address these issues, we have applied 2 distinct protocols previously established for hESCs [3,5] and derived HLCs from human iPSCs to determine whether iPSCs are capable of adopting a similar hepatic fate as

¹Molecular Embryology and Aging Group, Department of Vertebrate Genomics, Max Planck Institute for Molecular Genetics, Berlin, Germany.

²The Stem Cell Unit, Department of Anatomy, College of Medicine, King Saud University, Riyadh, Saudi Arabia.

hESCs. In addition, as the future utilization of these cells for *in vitro* toxicity tests and regenerative medicine will require detailed understanding of their transcriptomes, we have performed a critical transcriptome comparison between hESC- and iPSC-derived hepatocytes.

The analysis of the HLC transcriptomes revealed a broad spectrum of molecular cascades involving cell surface receptors, transcriptional regulators, cytochromes, and associated signaling pathways known to be active during hepatogenesis. Most importantly, hESC- and iPSC-derived HLCs showed vast transcriptional similarities as well as potentially relevant differences when compared to fetal liver and adult hepatic progenitors. We believe that these findings are vital to the refinement of efficient protocols for the eventual derivation of highly functional patient-specific HLCs that could be suitable for either cell replacement therapies or screens for drug toxicity.

Materials and Methods

Cell culture

hESC lines H1 and H9 (WiCell Research Institute) from passage 39 to 66 were maintained under sterile conditions in a humidified incubator in a 5% CO₂–95% air atmosphere at 37°C (INNOVA CO-170 Incubator; New Brunswick Scientific). In a routine culture, cells were maintained on Matrigel® in conditioned media [19]. Before initiating differentiation, cells were washed with phosphate-buffered saline (PBS) without Ca²⁺Mg²⁺ (Gibco, Invitrogen). Human iPSCs were previously generated [20]. In the present study, 2 lines (iPS2 and iPS4) were used for HLC generation.

PHHs (Ready Heps™ Fresh Hepatocytes; Lonza, 65-year-old male of Asian origin), hepatocellular carcinoma (HepG2, ATCC, and HB-8065; LGC Promochem), and human foreskin fibroblasts (HFF1, ATCC, and CRL-2429; LGC Promochem) cells were used as positive and negative controls, respectively, for the hepatocyte functional assays and immunocytochemistry. HepG2 and HFF1 cells were cultured in Dulbecco's modified Eagle's medium (DMEM) (high glucose; Gibco, Invitrogen) supplemented with fetal bovine serum [(10% (v/v); Biochrom AG, Berlin), 200 mM L-glutamine [1/100 (v/v); Gibco, Invitrogen], and penicillin–streptomycin [1/100 (v/v); Gibco, Invitrogen].

Differentiation into HLCs

The derivation of HLCs from the hESC lines H1 and H9 followed protocols described by Hay et al. [5] and Agarwal et al. [3]. iPSC lines (iPS2 and iPS4) used for the differentiation were between passage 16 and passage 20. Differentiation was initiated when cells reached 60%–70% confluence. RNA samples were extracted after each step of the differentiation protocol to examine the activation of endoderm and hepatic-associated genes. In addition, 2 iPSC lines (iPS2 and iPS4) were differentiated according to the Hay et al. protocol. On day 18, the cells were harvested for RNA isolation or used for immunofluorescence analysis and functional tests.

Real-time-polymerase chain reaction analysis

Using the RNeasy™ Mini Kit (Qiagen), total RNA was isolated from cells possessing hepatocyte-like morphologies.

This was achieved by scrapping off from the plate the cells that did not possess hepatocyte-like morphologies. Reverse transcription was carried out as previously described [21]. Real-time (RT)-polymerase chain reaction (PCR) was carried out on the Applied Biosystems 7900 instrument. Each gene was analyzed in triplicate. Three biological replicates were used of samples collected through both differentiation protocols for both hESC lines (H1 and H9). For iPSC experiments 2 biological replicates were used. Relative mRNA levels were calculated using the comparative CT method (ABI instruction manual) and presented as a percentage of the biological controls (undifferentiated hESCs). mRNA levels were normalized using *GAPDH*.

Immunocytochemistry

Immunocytochemistry was performed as previously described [20]. Briefly, cells were washed fixed with 4% paraformaldehyde, permeabilized with 1% Triton X-100, and blocked in PBST containing 1% bovine serum albumin (Fraction V, 99% purity; Sigma) and 5% normal chicken serum (Vector Laboratories, Inc.). Primary and secondary antibodies were then applied and cells were finally incubated with DAPI solution (Molecular Probes, Invitrogen). Fluorescence was examined under the confocal microscope (LSM510 Meta; Zeiss). Primary and secondary antibodies used are listed in Supplementary Table S1 (Supplementary Data are available online at www.liebertonline.com/scd).

Functional assays for HLCs

Periodic Acid-Schiff (PAS) Staining System (Sigma-Aldrich) was applied to identify glycogen storage. Cells were fixed with 4% paraformaldehyde for 15 min and stained according to manufacturer's instructions. Cellular uptake and release of indocyanine green (ICG; Cardiogreen, ICG; Sigma) [22,23] was performed to confirm the presence of albumin in hESC-derived HLCs and ability to uptake and excrete substances. Stock solution (5 mg/mL) of reagent was prepared in DMSO (Sigma) and freshly diluted in culture media to 1 mg/mL. For the initial experiments, hESCs were incubated in culture media supplemented with ICG for 30 min at 37°C. The cells were washed with PBS and uptake of dye was documented. The release of ICG was examined after 6 h. Subsequently, for both hESCs and iPSCs-HLCs (incubated with 1 mg/mL of ICG at 37°C for 2 h) excretion of ICG after 6 h was observed in some extent; however, we observed that the compound had been completely excreted the next day. Thus, we used the latter time point for our final comparison between iPSC- and hESC-derived HLCs. Undifferentiated hESCs and iPSCs were applied as a control and were negative for both, PAS staining and ICG uptake (Supplementary Fig. S1). PHHs were used as a positive control. The results of both assays were examined under an Olympus CK2 phase-contrast microscope and representative morphology was recorded at a magnification of ×50 using a Canon 300D digital camera.

In addition, urea secretion was quantified by a colorimetric assay QuantiChrom™ Urea Assay Kit (DIUR-500 BioAssay Systems) following the manufacturer's instructions. The assay detects urea directly by using substrates that specifically bind urea. Urea assays were carried out in 96-well plates, and

concentrations were measured using a plate reader. Urea production by the cells was quantified in 24 h conditioned medium from HepG2, iPSC2-HLCs_P1, iPSC4-HLCs_P1, hESCs-HLCs_P1, hESCs-HLCs_P2, and PHHs (7×10^5 cells). Medium from definitive endoderm-differentiated hESCs (hESCs-DE) was used as a negative control. Two biological replicates for each sample were analyzed. The levels of urea are presented as a percentage, considering measured levels of urea in mg/dL/24 h for 7×10^5 of PHHs as 100%.

Illumina BeadChip hybridization

Chip hybridizations have been performed as previously described [21]. We hybridized the following samples in biological triplicates—Protocol 1 (P1) [5]: H1 cell line passage 53 (hESCs_P1, control), hepatocyte-like cells (hESCs-HLCs_P1); Protocol 2 (P2) [3]: H1 cell line passage 60 (hESCs_P2, control), hepatocyte-like cells (hESCs-HLCs_P2). iPSCs (iPSC2 and iPSC4) and HLCs-iPSCs_P1 were hybridized as 2 biological

replicates. Two technical replicates (4 arrays) of RNA from fetal human liver (Stratagene, MVP™ Total RNA: tissue from single male donor, 18th week of gestation) were hybridized. The male RNA was analyzed since H1 hESC line used to generate HLCs is as well of male origin and iPSCs have been generated from male fibroblasts.

Data reproducibility was demonstrated by clustering of all hybridized samples and correlations of the biological replicates. All biological replicates in each group clustered together and the correlations coefficients (0.9835–0.9981) indicate a high degree of correlation between samples (data not shown).

Data analysis and statistical methods

Raw data obtained using the manufacturer's software BeadStudio 3.0.19.0. was imported into the Bioconductor environment [24] and quantile normalized using the bioconductor package Beadarray [25]. Pair-wise Pearson

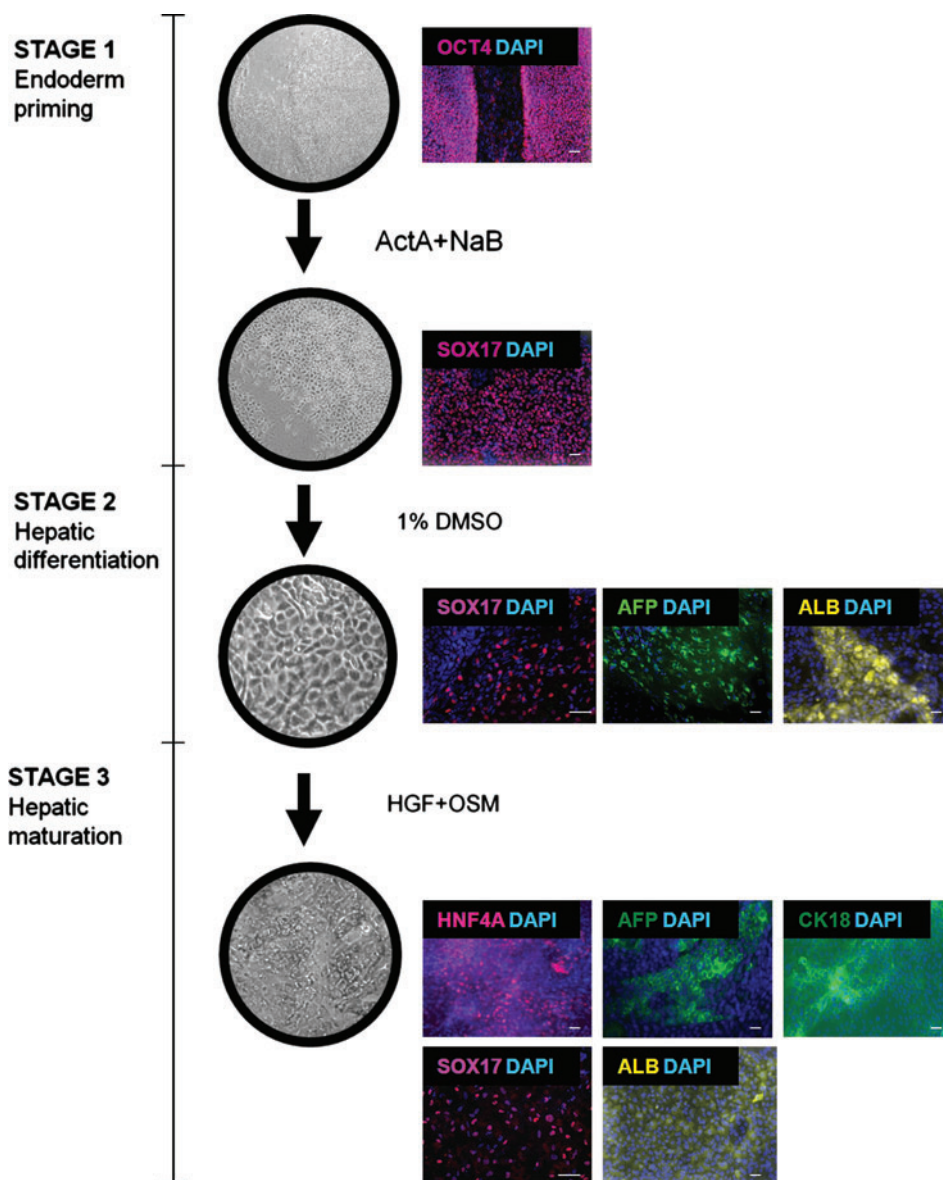


FIG. 1. Schematic illustration of the hepatic differentiation protocol [Protocol 1(P1)]. Phase-contrast images showing morphological changes during the progression of the protocol. Immunocytochemistry showing expression of various markers during the differentiation process. Scale bar = 10 μm. Color images available online at www.liebertonline.com/scd.

correlation coefficients were calculated for all samples. Variance and cluster analyses were performed using the R environment [26]. Filtering and compilations of data were carried out using MS Excel. Differential gene expression and analysis of variance (ANOVA) analyses were performed using the TIGR-MEV [27]. Differential gene expression was

calculated between all groups by the ANOVA analysis; P values were calculated based on F-distribution, with a critical P value of 0.05. For the ANOVA analysis, we created 2 separated contrast matrices for the P1 samples and P2 samples, respectively. The fetal liver samples were added to both groups. Based on these results, for each gene we obtained P

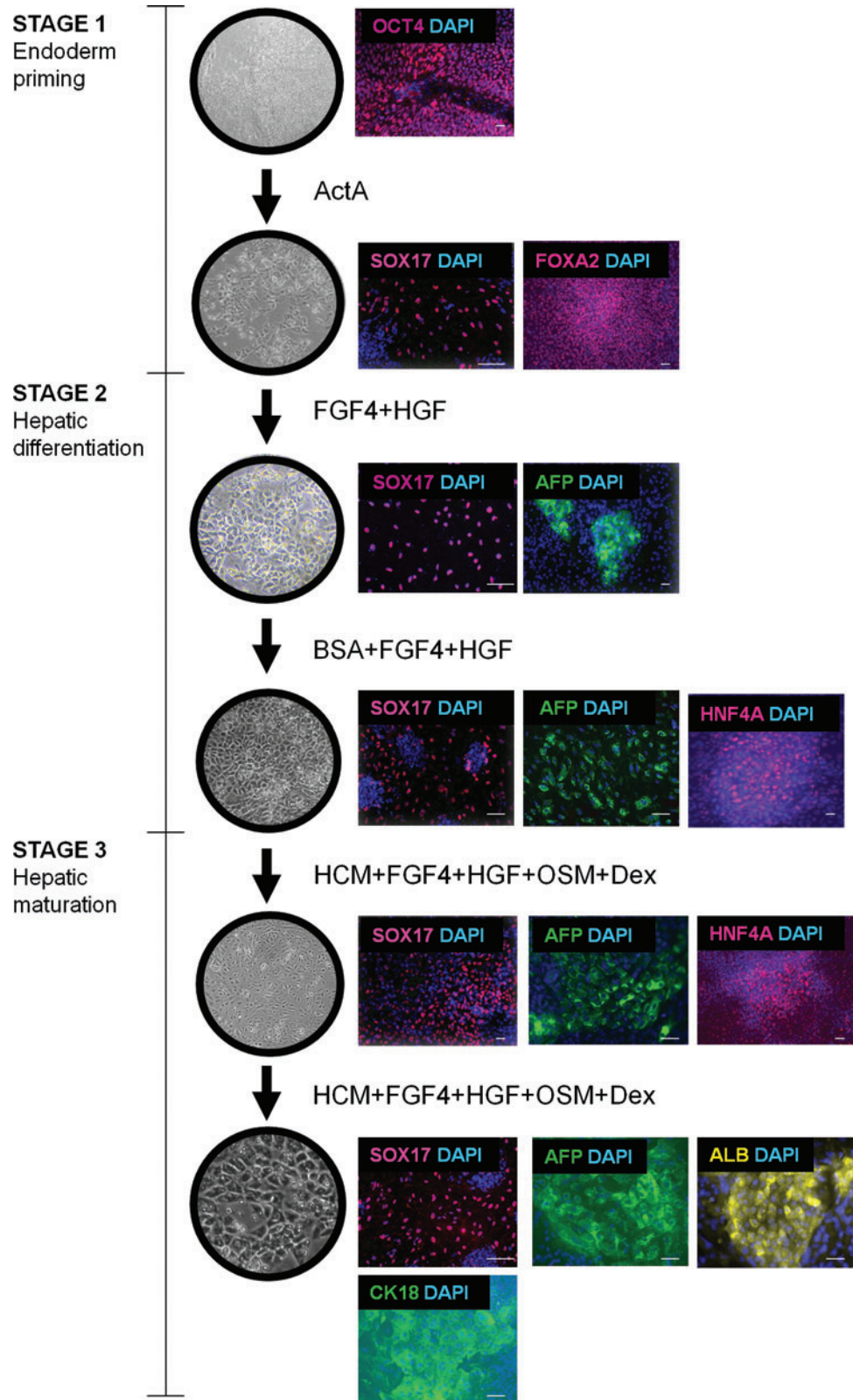


FIG. 2. Differentiation of human embryonic stem cells (hESCs) to hepatocyte-like cells (HLCs) [Protocol 2 (P2)]. Schematic illustration of the successive steps of the differentiation protocol. Phase-contrast images of differentiating cells and immunofluorescence analysis of the expression of specific marker proteins. Scale bar = 10 μ m. Color images available online at www.liebertonline.com/scd.

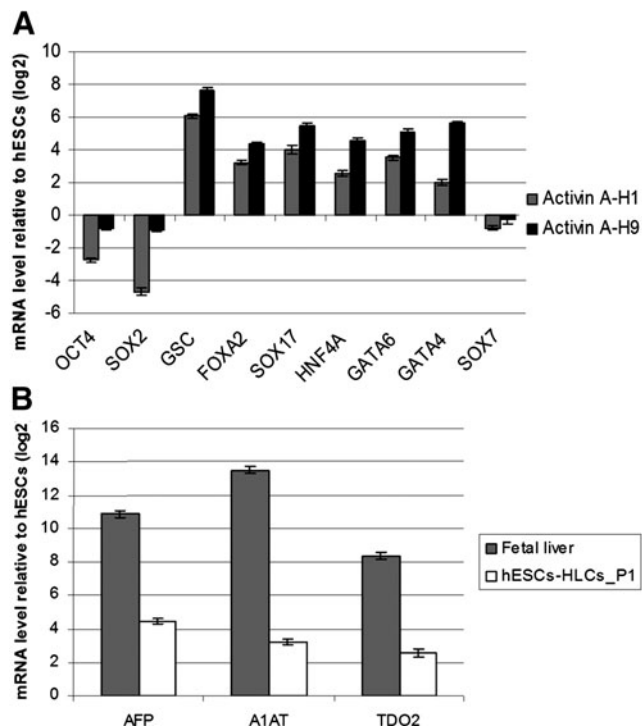


FIG. 3. Quantitative real-time (RT)-polymerase chain reaction (PCR) analysis of induced hepatocyte markers upon hESC differentiation. Analysis of **(A)** definitive endoderm and **(B)** hepatocyte marker gene expression by RT-PCR in definitive endoderm (DE; Activin A-treated) and HLCs derived from hESCs according to the 2 protocols. The error bars indicate the standard errors of the mean.

values that indicate the magnitude of gene expression variation throughout the samples of the tested group. Additionally, a list of genes expressed in human liver progenitors (HLPs) generated by us [21] has been used.

Differentially expressed genes were further filtered according to Gene Ontology terms or mapped to KEGG pathways using DAVID 2008 (<http://david.abcc.ncifcrf.gov>) [28,29]. For analysis, we used Illumina Gene IDs represented by the corresponding chip oligonucleotides as input. To examine potential interactions between 115 genes common between hESC- and iPSC-derived HLCs we have applied the STRING tool (<http://string-db.org/>) [30] to generate protein-protein interaction networks.

All original gene array files are available from the Gene Expression Omnibus (GEO) database (www.ncbi.nlm.nih.gov/geo/) (accession no. GSE25744).

Results

Differentiation of hESCs into HLCs using 2 independent multistage protocols

We have adopted 2 published differentiation protocols P1 [5] and P2 [3], which involved a DE induction step and sequential treatments of the derived DE cells with cytokines essential during hepatogenesis in vivo. We observed constant changes in morphology of hESCs from the undifferentiated stage (small cell sizes, defined colony borders) through to the DE stage (less dense, flatter cells) to HLCs (Figs. 1 and 2). For both protocols immunocytochemical analyses (Figs. 1 and 2) and real-time RT-PCR (Fig. 3) were further employed to confirm the extent of differentiation. As presented in Figs. 1 and 2, the differentiation did not give rise to a homogenous population of cells. Immunocytochemical analysis of PHHs was performed to better observe the extent of differentiation of both ESCs and iPSCs (Fig. 4).

To study the functionality of hESC-derived HLCs, we examined glycogen storage using PAS, and the ability of uptaking and excreting compounds by using ICG (Fig. 5A). In contrast to fibroblasts, HLCs exhibited glycogen storage capabilities and demonstrated the competence of uptake and

Primary Human Hepatocytes (PHH)

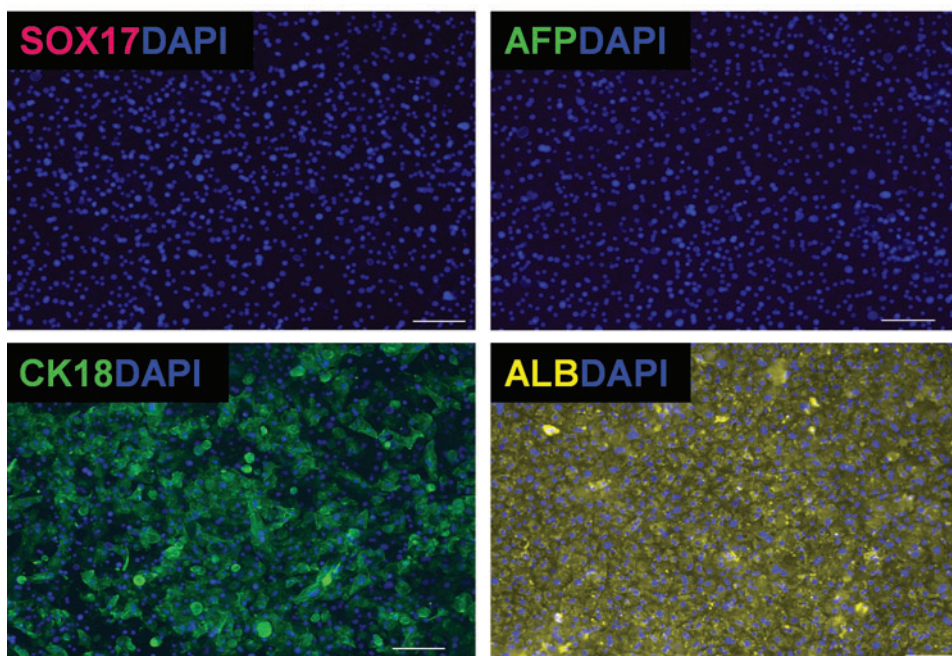
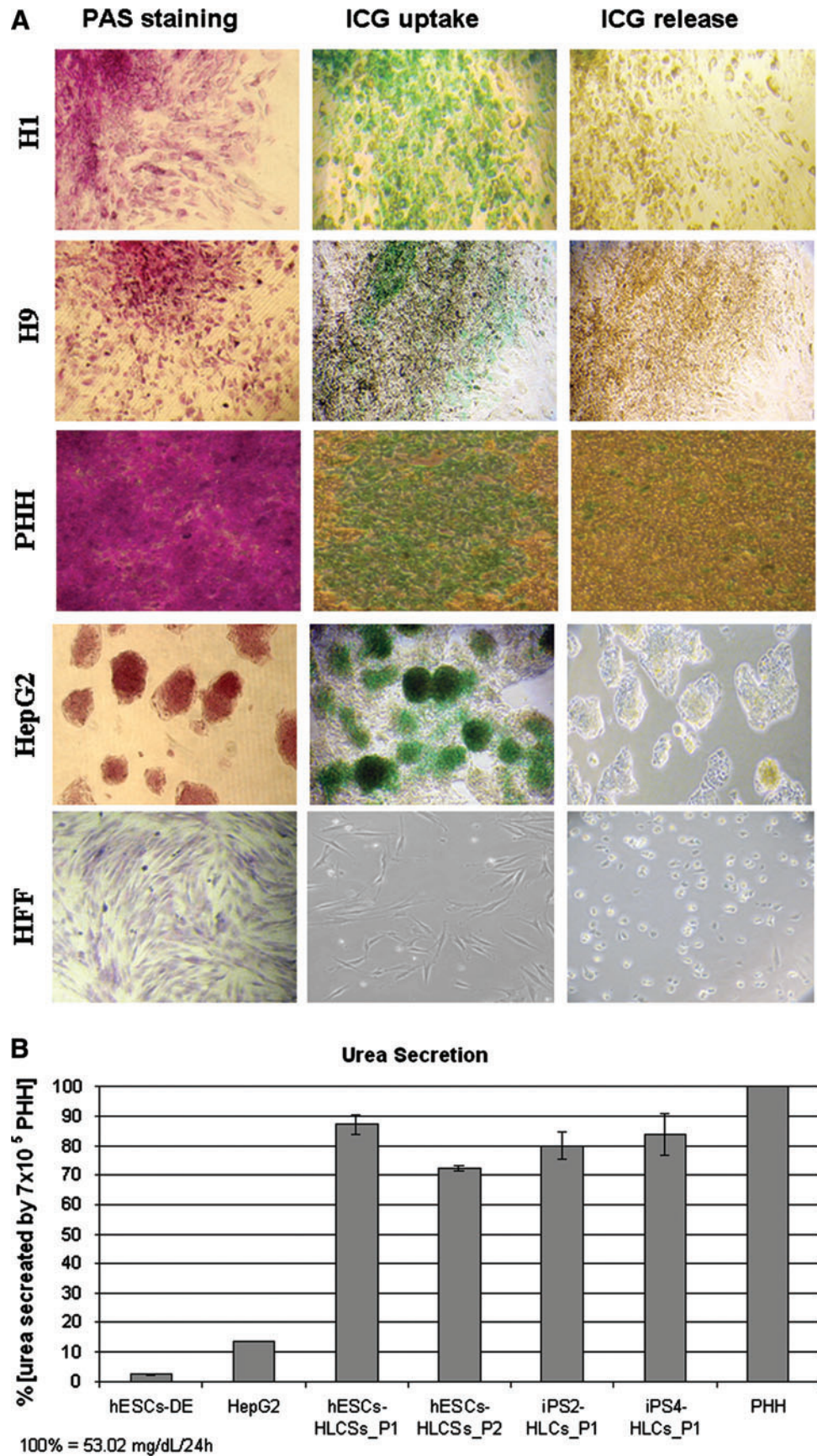


FIG. 4. Immunocytochemical analysis of primary human hepatocytes (PHHs). Immunostaining analysis was used to confirm the expression of markers that define adult hepatocytes (ALB and CK18) and the lack of expression of definitive endoderm marker (SOX17) and fetal liver marker [α -fetoprotein (AFP)] in human mature hepatocytes. Scale bar = 100 μ m. Color images available online at www.liebertonline.com/scd.

FIG. 5. HLCs exhibit hepatocyte-like functions. **(A)** Periodic acid-Schiff (PAS) assay was performed on hESC-derived HLCs (H1 and H9), HepG2, and human foreskin fibroblast (HFF). Glycogen storage is demonstrated by pink or dark red-purple staining within the cytoplasm. hESCs at the end of the differentiation protocols, PHH, HepG2 (positive controls), and HFF (negative control) were examined for their ability to take up indocyanine green (ICG) and release it 6 h later. The results of both assays were examined under an Olympus CK2 phase-contrast microscope and at a magnification of $\times 50$ using a Canon 300D digital camera. **(B)** Analysis of urea production in hESCs-DE, HepG2, iPS2-HLCs_P1, iPS4-HLCs_P1, hESCs-HLCs_P1, hESCs-HLCs_P2, and PHHs (7×10^5 cells). Two biological replicates of each sample were analyzed. The levels of urea are presented as a percentage, considering measured levels of urea in mg/dL/24h for 7×10^5 of PHHs as 100% (100% = 53.02 mg/dL/24h). The error bars indicate the standard errors of the mean. Color images available online at www.liebertonline.com/scd.



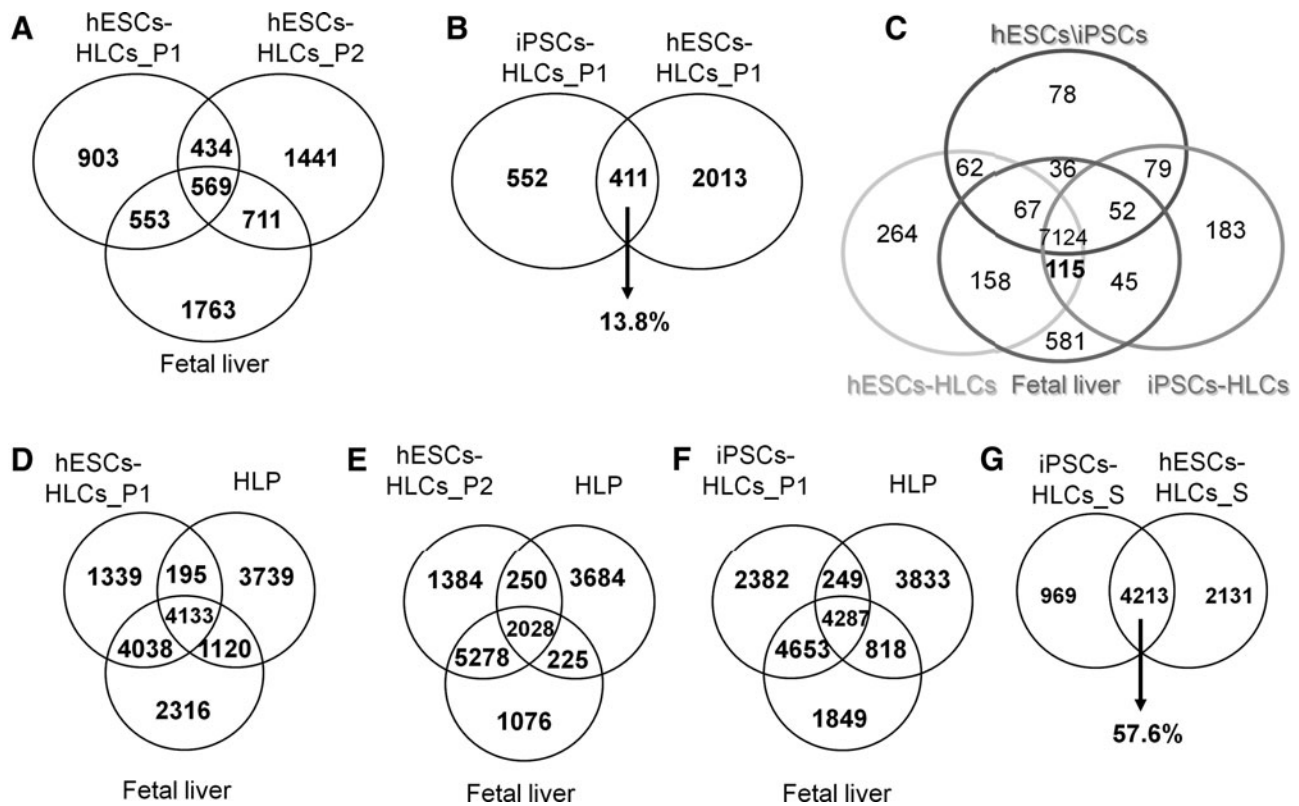


FIG. 6. Venn diagram illustrating the overlap of genes expressed in common between HLCs, fetal liver, and human liver progenitors (HLPs). **(A)** The Venn diagram illustrates the overlap of target gene lists of HLCs derived from hESCs and fetal liver. **(B)** Venn diagram showing the overlap between HLCs derived from hESCs and induced pluripotent stem cells (iPSCs) applying the same protocol. **(C)** Venn diagram showing the overlap between hESC-HLCs, iPSC-HLCs, and fetal liver. **(D–F)** Venn diagrams presenting the overlap between hESC-HLCs, iPSC-HLCs, fetal liver, and HLPs. **(G)** Venn diagram presenting the overlap between HLCs generated from hESCs and iPSCs by Si-Tayeb et al. [9].

excretion of ICG. For both functional tests, the PHHs and hepatocellular carcinoma cell line (HepG2) were used as positive controls.

In addition, hESC-HLCs_P1, hESC-HLCs_P2, iPSC-HLCs_P1, and iPSC-HLCs_P1 exhibited a similar pattern of urea production. The levels of urea are presented as a percentage, considering measured levels of urea in mg/dL/24h for 7×10^5 of PHHs as 100% (Fig. 5B).

Global gene expression analysis of hESC-HLCs obtained with the 2 differentiation protocols

hESC-HLCs derived with P1 had 2,459 genes significantly upregulated in comparison to undifferentiated hESCs ($P < 0.05$, detection $P < 0.01$, ratio > 1.5). In HLCs derived with P2, 3,155 genes were upregulated compared to undifferentiated cells.

To find potential common genes, biological processes and related pathways, data sets from 2 independently derived HLCs and fetal liver were compared. The male fetal liver RNA was used as a reference in accordance with male origin of H1 hESC line and reprogrammed fibroblasts.

The Venn diagram in Fig. 6A illustrates that among the significantly upregulated genes, there are 569 genes expressed in all 3 analyzed samples. Identified genes known to be implicated in hepatic function are shown in Table 1. Tissue ex-

pression signatures enriched in HLCs is presented in Table 2. hESC-HLCs_P1 and iPSC-HLCs_P1 (derived applying the same differentiation protocol) possess expression signatures closely related to pancreas and adrenal cortex, whereas the hESC-HLCs_P2 tissue expression signature is similar to fetal liver and appendix.

Comparative differentiation of hESCs and iPSCs into HLCs

We then addressed whether the culture conditions applied to derive HLCs from hESCs are also as efficient in differentiating iPSCs. Both protocols were performed simultaneously; therefore, we could not anticipate which of the 2 protocols would yield a higher efficiency. Indeed, all articles published so far used only a specific protocol and a detailed comparison between different protocols have yet to be done. Based on published works, it seemed that both protocols performed equally in generating HLCs. P1 [5] appeared more suitable for larger scale in vitro toxicology assays, since it was less complex and required addition of a fewer number of recombinant proteins. Hence, we adopted this also for the generation of HLCs from the 2 iPSC lines, iPSC2 and iPSC4.

The lines iPSC2 and iPSC4, and the hESC line H1 were simultaneously differentiated. Interestingly, we noted higher levels of cell death in iPSC2 and iPSC4 than in H1. This suggests

TABLE 1. HEPATOCYTE-RELATED GENES

Genes upregulated in hESCs-HLCs_P1_P2 and fetal liver <i>FOXA1, LEAP2, MUC1, SERPINA3, SERPINC1, CYP51A1, SERPINF1, SERPING1, SULT1C2, ALDH1A2, ALDH5A1</i>
Genes upregulated in hESCs-HLCs_P1 and fetal liver <i>ALDH1L1, ALDH3A, GSTA4, GSTM4, LHX2, RXRA</i>
Genes upregulated in hESCs-HLCs_P2 and fetal liver <i>ALB, AFP, TTR, CEBPA, GATA5, SERPINA1, FGA, FGB, FGG</i>
<i>SERPINF2, GSTA1, GSTA2, GSTK1, ABCD1, ABCF3, ABCC5</i>
<i>APOA2, APOB, APOC3, ABCC3</i>
Genes upregulated in hESCs-HLCs_P1 and not iPSCs-HLCs_P1 <i>ITIH5, SERPINA1, SERPINA3, CYP19A1, MGST3, MAOA, CYP1A1, CYP11A1, ATF4, C3, HSD17B1, SULT1A2, GSTA1</i>
Genes upregulated in iPSCs-HLCs_P1 and not hESCs-HLCs_P1 <i>CYP46A1, CYP26A1, GPX3, GSTM1, GSTM2, EPHX1, SMARCA1</i>

Examples of genes involved in hepatocyte physiology and upregulated in hESCs-HLCs, iPSCs-HLCs, and fetal liver.

AFP, α -fetoprotein; hESCs, human embryonic stem cells; HLCs, hepatocyte-like cells; iPSCs, induced pluripotent stem cells.

that iPSCs might have a higher number of cells unable to fully differentiate, possibly due in part to the random viral integration known to occur in virally generated iPSCs [10,11]. Given this high mortality rate, cells were not split during the course of the differentiation process. Gradually, cells displayed morphological changes from a spiky to a polygonal shape (Fig. 7A). On day 18, both hESC and iPSCs and derived HLCs (iPSCs-HLCs) had cellular foci exhibiting features of human hepatocytes, including typical polygonal shape, and expression of hepatocyte markers such as α -fetoprotein and ALB (Fig. 7B).

To investigate the functional capabilities of iPSCs-HLCs, we have performed identical tests like for hESCs-HLCs (Figs. 5B and 7C). Both HLCs exhibited comparable functionality, suggesting that different pluripotent cell sources could be able to generate functionally similar HLCs. Finally, the expression levels of several hepatocyte markers were analyzed by real-time (RT)-PCR. All markers were upregulated in both iPSC- and hESC-derived HLCs compared to undifferentiated cells (Fig. 7D, E). The level of induction was not as high as in fetal liver, likely due to the fact that fully matured HLCs were only present in cellular foci and thus under-represented with respect to the total amount of cells.

Comparative global gene expression analysis between hESCs-HLCs and iPSCs-HLCs

Comparative gene expression analysis was performed in hESC- and iPSC-derived HLCs. As expected, the clustering showed high diversity between fetal liver and HLCs (Supplementary Fig. S2A). The transcriptomes of HLCs were still far from fetal liver but are closer to each other than to undifferentiated hESCs (Supplementary Fig. S2B).

A transcriptional comparison between hESCs-HLCs and iPSCs-HLCs employing the same differentiation protocol (P1) revealed 411 genes in common (Fig. 6B). Interestingly, some liver-related genes were specifically enriched within ESCs-HLCs (such as *CYP19A1*, *CYP1A1*, and *CYP11A1*),

whereas others were significantly enriched in iPSCs-HLCs only, including *CYP46A1* and *CYP26A1* (Table 1). Among genes upregulated ($P < 0.05$, detection $P < 0.01$, ratio > 1.5) in both hESCs-HLCs (both P1 and P2) and iPSCs-HLCs in comparison to undifferentiated cells, we specifically focused on transcription factors, cytochromes, and cell surface receptors. The highly upregulated (fold changes between 4.5 and 889.97) genes in each category are presented in Table 3. Supplementary Table S2A–F presents the entire results of this analysis for hESCs-HLCs_P1, hESCs-HLCs_P2, and iPSCs-HLCs_P1, respectively.

To date, the array analysis of hepatocyte-like cells derived from hESCs (hESCs-HLCs_S) and iPSCs (hESCs-HLCs_S) has been performed only by Si-Tayeb et al. [9] employing Gene-Chip Human Genome U133 Plus 2.0 arrays (Affymetrix). We have analyzed their data to identify genes upregulated upon differentiation (the level of significance was set to 0.05 and expected a fold change of at least 1.5). The analysis revealed that 5,182 genes were upregulated in iPSCs-HLCs compared to iPSCs and 6,344 genes were upregulated in hESCs-HLCs compared to hESCs. The HLCs generated from both hESCs and iPSCs shared the expression of 4,213 genes (Fig. 6G and Supplementary Table S3). This analysis allowed us to fully confirm the transcriptional differences between HLCs generated from hESCs and iPSCs. The HLCs generated from hESCs and iPSCs by Si-Tayeb et al. shared 57% of upregulated genes, whereas the HLCs derived according to P1 in our hands shared 18% of upregulated genes (Fig. 6B, G). These findings highlighted the importance of global transcriptional studies but also differences that can be attributed to the different microarray platforms used by us (Illumina) and them (Affymetrix).

The comparison of transcriptomes of hESC- and iPSC-derived HLCs and fetal liver (Fig. 6C) revealed that these cells express a core of 115 genes in common. Among these, 9 were transcription factors, 1 cytochrome, and 11 cell surface receptors (Table 4). Protein interaction network of these genes is presented in Supplementary Fig. S3. Interactions were not predicted for 74 of the 115 genes, thus highlighting the novelty of our findings.

However, interactions between genes known to be expressed in the liver like *GPX1* and *GSTM3* were identified. Interestingly, interaction between proteins involved in fatty acids synthesis and elongation (*MCAT* and *OXSM*) were also identified.

Pathway analysis revealed biological processes common in hESC-HLCs_P1 and fetal liver include lipid metabolism, steroid metabolism, lipid transport, and the complement and coagulation cascade pathway (Table 2). The biological processes of fatty acid and alcohol metabolism and the pathways of steroids and polyunsaturated fatty acid biosynthesis were common between hESC-HLCs_P2 and fetal liver. Lipid, sterol, and alcohol metabolic processes were found as common between iPSCs-HLCs and fetal liver (Table 2).

Finally, we also included in the comparison adult HLPs [21] (Fig. 6D–F). Interestingly, we observed that HLCs derived from ESCs and iPSCs shared more transcripts in common with fetal liver than with HLPs. Moreover, among the genes expressed in common between HLCs and HLPs, we detected the presence of HLP marker genes. As we previously demonstrated, these genes (such as *VGLL* and *EpCAM*) are expressed in common only in the progenitor

TABLE 2. PATHWAYS ANALYSIS IN HUMAN EMBRYONIC STEM CELLS AND INDUCED PLURIPOTENT STEM CELL-HEPATOCYTE-LIKE CELLS

<i>hESCs-HLCs_P1 and fetal liver</i>		
<i>Term</i>	<i>Count</i>	<i>P value</i>
<i>GO-BP</i>		
Response to wounding	33	3.84E-06
Response to chemical stimulus	38	4.08E-05
Lipid metabolic process	43	1.02E-04
Aromatic compound metabolic process	13	3.95E-04
Steroid metabolic process	15	9.06E-04
Lipid transport	11	1.10E-03
<i>Pathways</i>		
Complement and coagulation cascades	10	3.09E-03
<i>Tissue expression signature</i>		
Pancreas	888	2.28E-116
Adrenal cortex	631	7.62E-68
<i>hESCs-HLCs_P2 and fetal liver</i>		
<i>GO-BP</i>		
Metabolic process	328	1.78E-03
Fatty acid metabolic process	16	1.83E-03
Cellular metabolic process	296	2.34E-03
Cellular lipid metabolic process	36	4.16E-03
Alcohol metabolic process	20	1.33E-02
<i>Pathways</i>		
Biosynthesis of steroids	6	7.08E-04
Polyunsaturated fatty acid biosynthesis	5	1.71E-03
<i>Tissue expression signature</i>		
Fetal liver	1,121	7.58E-101
Appendix	1,055	3.34E-81
<i>iPSCs-HLCs_P1 and fetal liver</i>		
<i>GO-BP</i>		
Lipid metabolic process	38	3.91E-10
Sterol metabolic process	14	2.19E-09
Alcohol metabolic process	24	6.26E-08
Cholesterol metabolic process	10	7.11E-06
Response to wounding	20	2.50E-04
Fatty acid metabolic process	11	6.10E-04
Monocarboxylic acid metabolic process	13	1.45E-03
<i>Pathways</i>		
Biosynthesis of steroids	7	7.31E-07
Biosynthesis of cholesterol	4	9.46E-04
ECM-receptor interaction	7	7.77E-03
Focal adhesion	11	8.67E-03
<i>Tissue expression signature</i>		
Adrenal cortex	279	2.09E-42
Pancreas	323	8.86E-35

Lists of overlapping GOs, pathways, and tissue signatures for genes common in hESCs and iPSCs-HLCs and fetal liver.
GO, gene ontology.

state, as their expression is lost in adult liver cells [31]. This would suggest that HLCs may not represent a mature hepatic state but rather an immature progenitor-like state.

Liver signature and cytochromes P450

Since one of the ultimate applications of HLCs is the in vitro hepatotoxicity test, we specifically looked at the ex-

pression of detoxifying enzymes. The most abundant CYP in human liver, *CYP3A4*, and the major cytochromes in fetal liver, *CYP3A7* and *CYP3A5*, were expressed in HLCs but less than 1.5-fold upregulated in comparison to undifferentiated cells. This may imply that these cytochromes might be successfully induced upon stimulation of the cells with appropriate stimuli. On the other hand, the expression of other enzymes such as, *CYP46A1* and *CYP26B1*, was significantly

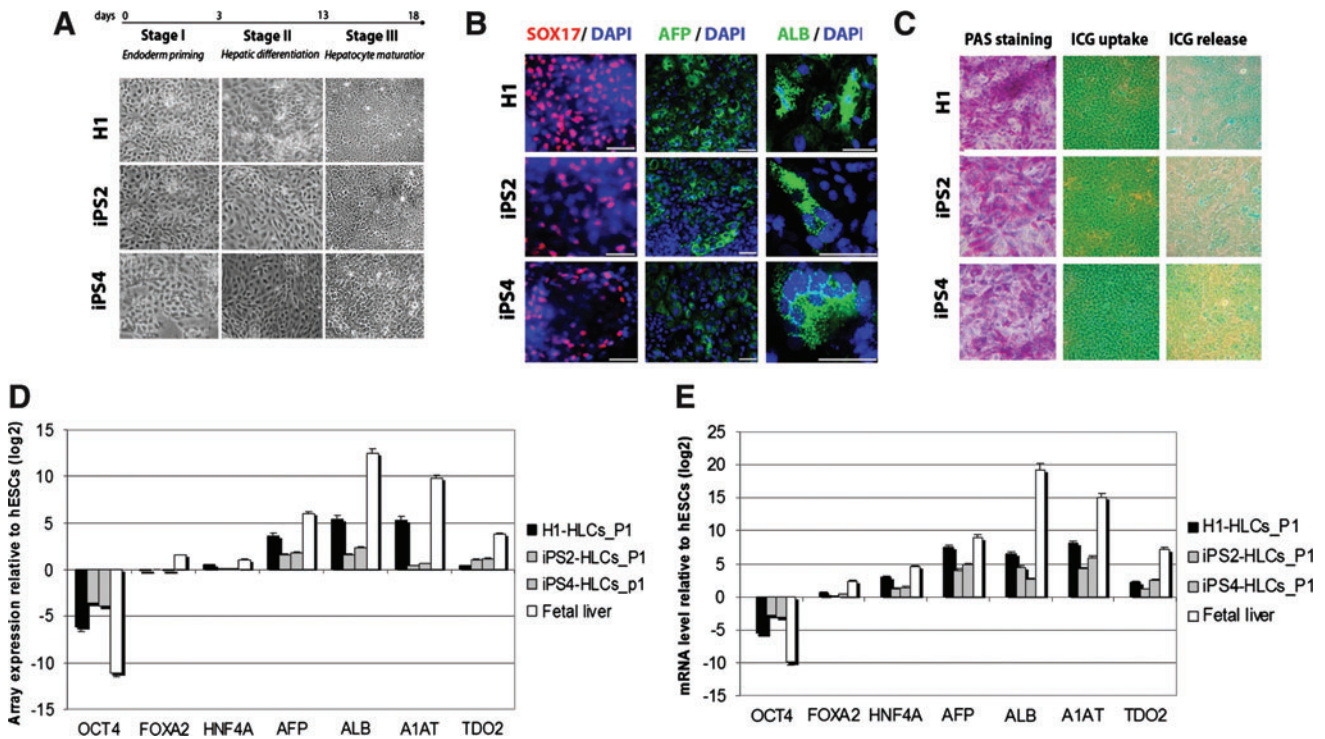


FIG. 7. Generation of HLCs from iPSCs. HLCs were generated from hESC H1 line and from iPSC iPS2 and iPS4 lines using a 3-step protocol previously demonstrated in hESCs [5], illustrated in Fig. 1 (P1). **(A) Upper panel,** general outline of the 3-step procedure is depicted. **Lower panel,** pictures showing the cellular morphology at the end of each stage. **(B)** Immunofluorescence staining for the endoderm marker SOX17 and the hepatocyte markers AFP and albumin (ALB) in HCLs derived from H1, iPS2, and iPS4. Scale bar = 10 μ m. **(C)** Functional assays in HLCs. Glycogen deposits were observed using the PAS staining kit. The ability to uptake and release substances was monitored using 1 mg/mL of the ICG dye. The uptake was determined after 2 h of incubation, whereas the release was detected 18 h later. The results of both assays were examined under an Olympus CK2 phase-contrast microscope and at a magnification of $\times 50$ using a Canon 300D digital camera. Analysis of hepatocyte marker expression by Illumina array **(D)** and RT-PCR **(E)** in HLCs derived from H1 (H1-HLCs_P1) and HLCs derived from iPS2 and iPS4 (iPS2-HLCs_P1 and iPS4-HLCs_P1). Color images available online at www.liebertonline.com/scd.

upregulated in all HLCs compared to undifferentiated cells (fold change between 1.53 and 238.89) (Table 3). The heat map presented in Fig. 8A highlights the diversity between cytochromes expressed in fetal liver and those not expressed and specific to the adult liver.

Expression of *CYP1A1*, which is generally detectable in fetal liver and not in adult tissues, was 58-fold upregulated in hESCs-HLCs_P1. In contrast, *CYP1A2*, which does not play a role in fetal xenobiotic metabolism and is absent during the fetal and neonatal periods, was not significantly upregulated in any of the HLCs. In addition, although members of the CYP2 gene family are generally not expressed at the high levels in the adult liver, *CYP2E1*, which is known to be active in the metabolism of organic solvents, was found upregulated in both hESCs-HLCs_P1 and iPSCs-HLCs_P1 in comparison to undifferentiated cells [32].

The pattern of expression of genes crucial for drug metabolism process, which include drug transporters and phase II metabolizing, appeared very similar in both hESC- and iPSC-derived HLCs (Table 5). However, the expression levels of many phase I and II enzymes were lower in HLCs than in fetal liver. Thus, HLCs may have attained a state exhibiting many hepatic functions but probably incapable of fully recapitulating in vivo liver activities.

Finally, we sought to determine the liver-specific signature of HLCs (Fig. 8B) [33]. Transcriptional differences between hESCs-HLCs_P1, iPSCs-HLCs_P1, and hESCs-HLCs_P2 could be observed. The expression pattern of hESCs-HLCs_P1 and iPSCs-HLCs_P1 was more similar to each other than to hESCs-HLCs_P2 (and hence more similar to fetal liver when we concentrate only on genes assigned as a liver signature). In all 3 HLC samples analyzed, high expression of *SERPINA3*, *SERPINF1*, *SERPINB1*, *SERPING1*, and *SERPINH1* was observed. This is of particular interest because the SERPIN gene family are involved in the inhibition of serine proteases in the plasma and regulation of the complement cascade [34]. The SERPINs are abundantly secreted by liver and play a key role in controlling blood coagulation. Moreover, the complement and coagulation pathway was found as a common pathway shared between hESCs-HLCs and fetal liver. The presence of many SERPIN genes among the highly expressed genes confirms the expression of genes important for liver function.

Discussion

Treatment of chronic liver diseases with transplantation surgery is currently undermined by the limited availability of donated organs. Moreover, the PHHs routinely used in

TABLE 3. HUMAN EMBRYONIC STEM CELL–HEPATOCYTE-LIKE CELLS VERSUS INDUCED PLURIPOTENT STEM CELL–HEPATOCYTE-LIKE CELLS

<i>hESCs-HLCs_P1</i>			
<i>Gene name</i>		<i>P value</i>	<i>Ratio (HLCs/hESCs)</i>
<i>Transcription factors</i>			
<i>HIF3A</i>	Homo sapiens hypoxia inducible factor 3, alpha	5.14E-08	24.58
<i>ZBTB16</i>	Homo sapiens zinc finger and BTB domain containing 16	9.83E-09	20.65
<i>PLAGL1</i>	Homo sapiens pleiomorphic adenoma gene-like 1	3.95E-06	20.49
<i>CEBPD</i>	Homo sapiens CCAAT/enhancer binding protein delta	2.36E-10	20.28
<i>GCM1</i>	Homo sapiens glial cells missing homolog 1	9.23E-13	19.67
<i>Cytochromes</i>			
<i>CYP19A1</i>	Homo sapiens cytochrome P450, family 19, subf. A, pp. 1	9.25E-14	238.89
<i>CYP1A1</i>	Homo sapiens cytochrome P450, family 1, subf. A, pp. 1	9.99E-16	58.01
<i>CYP1B1</i>	Homo sapiens cytochrome P450, family 1, subf. B, pp. 1	5.55E-16	13.15
<i>CYP11A1</i>	Homo sapiens cytochrome P450, family 11, subf. A, pp. 1	7.44E-15	9.45
<i>CYP2J2</i>	Homo sapiens cytochrome P450, family 2, subf. J, pp. 2	1.01E-12	4.52
<i>CYP2E1</i>	Homo sapiens cytochrome P450, family 2, subf. E, pp. 1	3.83E-04	3.40
<i>CYP51A1</i>	Homo sapiens cytochrome P450, family 51, subf. A, pp. 1	3.20E-05	1.70
<i>Cell surface receptors</i>			
<i>IL1RL1</i>	Homo sapiens interleukin 1 receptor-like 1	1.20E-13	137.89
<i>IL18R1</i>	Homo sapiens interleukin 18 receptor 1	2.00E-15	133.49
<i>CCR7</i>	Homo sapiens chemokine (C-C motif) receptor 7	9.25E-11	42.23
<i>GPBAR1</i>	Homo sapiens G protein-coupled bile acid receptor 1	4.06E-08	34.18
<i>OLR1</i>	Homo sapiens oxidised low density lipoprotein receptor 1	4.23E-10	25.65
<i>hESCs-HLCs_P2</i>			
<i>Transcription factors</i>			
<i>NR2F1</i>	Homo sapiens nuclear receptor subf. 2, group F, member 1	4.16E-14	889.97
<i>RUNX2</i>	Homo sapiens runt-related transcription factor 2	2.77E-05	347.30
<i>POU4F2</i>	Homo sapiens POU domain, class 4, transcription factor 2	4.12E-10	280.02
<i>HOXA5</i>	Homo sapiens homeobox A5	2.14E-08	276.71
<i>HOXA2</i>	Homo sapiens homeobox A2	9.59E-13	169.19
<i>Cytochromes</i>			
<i>CYP46A1</i>	Homo sapiens cytochrome P450, family 46, subf. A, pp. 1	6.61E-11	31.31
<i>CYP26B1</i>	Homo sapiens cytochrome P450, family 26, subf. B, pp. 1	1.62E-08	30.94
<i>CYP1B1</i>	Homo sapiens cytochrome P450, family 1, subf. B, pp. 1	7.97E-07	8.77
<i>CYP4V2</i>	Homo sapiens cytochrome P450, family 4, subf. V, pp. 2	1.11E-16	1.55
<i>CYP51A1</i>	Homo sapiens cytochrome P450, family 51, subf. A, pp. 1	4.65E-05	1.53
<i>Cell surface receptors</i>			
<i>NTRK2</i>	Homo sapiens neurotrophic tyrosine kinase, receptor, type 2	3.18E-10	746.16
<i>PTPRO</i>	Homo sapiens protein tyrosine phosphatase, receptor type, O	1.51E-11	141.78
<i>OSMR</i>	Homo sapiens oncostatin M receptor	1.56E-07	91.26
<i>GPR56</i>	Homo sapiens G protein-coupled receptor 56	5.08E-09	38.24
<i>GRIA2</i>	Homo sapiens glutamate receptor, ionotropic, AMPA 2	1.53E-07	17.06
<i>iPSCs-HLCs_P1</i>			
<i>Transcription factors</i>			<i>Ratio (HLCs/iPSCs)</i>
<i>HAND1</i>	Homo sapiens heart and neural crest derivatives expressed 1	8.01E-03	11.37
<i>HOXB5</i>	Homo sapiens homeobox B5	4.51E-02	9.00
<i>PRRX2</i>	Homo sapiens paired-related homeobox 2	4.33E-03	7.32
<i>NKX6-2</i>	Homo sapiens NK6 homeobox 2	2.34E-13	4.58
<i>CEBPD</i>	Homo sapiens CCAAT/enhancer binding protein delta	3.68E-38	4.55

(Table continued →)

TABLE 3. (CONTINUED)

<i>iPSCs-HLCs_P1</i>			
<i>Cytochromes</i>			
<i>CYP1B1</i>	Homo sapiens cytochrome P450, family 1, subf. B, pp. 1	8.22E-15	5.46
<i>CYP46A1</i>	Homo sapiens cytochrome P450, family 46, subf. A, pp. 1	6.27E-09	3.14
<i>CYP2E1</i>	Homo sapiens cytochrome P450, family 2, subf. E, pp. 1	4.17E-03	1.97
<i>CYP26B1</i>	Homo sapiens cytochrome P450, family 26, subf. B, pp. 1	4.89E-02	1.67
<i>Cell surface receptors</i>			
<i>PDGFRB</i>	Homo sapiens platelet-derived growth factor receptor, beta	3.36E-03	6.93
<i>ITGA11</i>	Homo sapiens integrin, alpha 11	2.79E-04	5.68
<i>ITGB4</i>	Homo sapiens integrin, beta 4	2.59E-03	5.22
<i>PDGFRA</i>	Homo sapiens platelet-derived growth factor receptor, alpha	3.04E-04	5.15
<i>GPER</i>	Homo sapiens G protein-coupled estrogen receptor 1	2.08E-25	4.78

List of transcription factors, cytochromes and cell surface receptors present among genes upregulated in hESC- and iPSC-derived HLCs.

drug toxicology assays possess several constraints, including heterogeneity and limited culture potential. Thus, stem cell (hESCs or iPSCs)-derived hepatocytes have the potential to represent a defined and renewable source for cell replacement therapies and drug screening assays.

In our article, we addressed the important issue of molecular similarities between hESC- and iPSC-derived HLCs. So far, 4 articles have been published describing the generation of

HLCs from iPSCs [6–9]. Overall, only one group [9] provided functional data (transplanted HLCs) and all mentioned publications compared hESC- and iPSC-derived HLCs mainly on the bases of the expression of few known liver-related genes. Thus, we believe that it is of high relevance to examine in detail the molecular similarities of hESC- and iPSC-derived HLCs. To this end, the use of transcriptomics technique has the potential to reveal common and specific signatures of

TABLE 4. FEATURES OF THE COMMON 115 GENES

<i>Gene name</i>	<i>Definition</i>	
	<i>Transcription factors</i>	
<i>CNOT7</i>	Homo sapiens CCR4-NOT transcription complex, subunit 7	
<i>MAF</i>	Homo sapiens v-maf musculoaponeurotic fibrosarcoma oncogene homolog	
<i>MEN1</i>	Homo sapiens multiple endocrine neoplasia I	
<i>RUNX1</i>	Homo sapiens runt-related transcription factor 1	
<i>TARDBP</i>	Homo sapiens TAR DNA binding protein	
<i>TBX2</i>	Homo sapiens T-box 2	
<i>ZHX1</i>	Homo sapiens zinc fingers and homeoboxes 1	
<i>ZNF187</i>	Homo sapiens zinc finger protein 187	
<i>ZNHIT3</i>	Homo sapiens zinc finger, HIT type 3	
<i>Cytochromes</i>		
<i>CYP26B1</i>	Homo sapiens cytochrome P450, family 26, subfamily B, polypeptide 1	
<i>Cell surface receptors</i>		
<i>ACVR1B</i>	Homo sapiens activin A receptor, type IB	
<i>ADRB2</i>	Homo sapiens adrenergic, beta-2-, receptor	
<i>ASGR2</i>	Homo sapiens asialoglycoprotein receptor 2	
<i>CCBP2</i>	Homo sapiens chemokine binding protein 2	
<i>EDG1</i>	Homo sapiens endothelial differentiation, sphingolipid G-protein-coupled receptor, 1	
<i>GPBAR1</i>	Homo sapiens G protein-coupled bile acid receptor 1	
<i>IL18R1</i>	Homo sapiens interleukin 18 receptor 1	
<i>KREMEN1</i>	Homo sapiens kringle containing transmembrane protein 1	
<i>PILRA</i>	Homo sapiens paired immunoglobulin-like type 2 receptor alpha	
<i>PTPRE</i>	Homo sapiens protein tyrosine phosphatase, receptor type, E	
<i>SPN</i>	Homo sapiens sialophorin (leukosialin, CD43)	

List of transcription factors, cell surface receptors, and cytochromes present among the 115 genes expressed in common between fetal liver and HLCs derived from both hESCs and iPSCs.

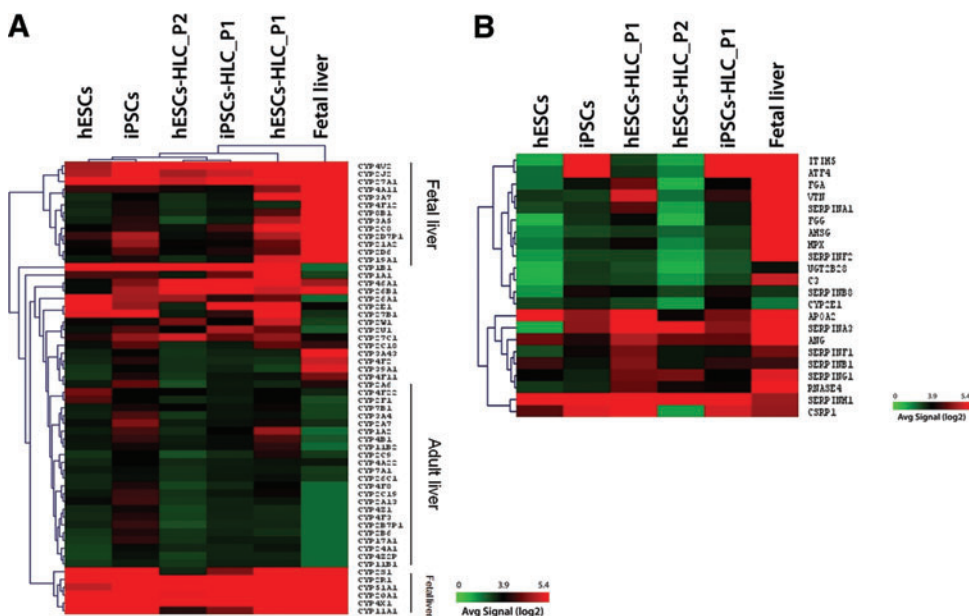


FIG. 8. Heat map of gene array analysis. **(A)** Hierarchical cluster dendrogram of cytochromes expression in hESCs, iPSCs, HLCs, and fetal liver. **(B)** Heat map presenting genes described in the literature as liver specific [33]. The heat maps are colored by LOG2 average expression signals according to the color key at the bottom. Genes and samples were clustered by similar expression pattern using an Euclidian distance measure. Color images available online at www.liebertonline.com/scd.

HLCs obtained from ESCs and iPSCs, by assaying the whole genome and not only the expression of genes already known and expected to be altered on the basis of prior knowledge. We believe that whole genome transcriptional analysis as we have conducted is obligatory if we are to understand the real potential of iPSCs-based liver regenerative medicine and toxicology.

In this work, we have applied and compared 2 distinct multistep protocols for the efficient derivation of HLCs from hESCs. Both protocols were able to recapitulate the progressive specification of DE and hepatocytes during development. However, detailed pathway analysis of global expression profile shows subtle differences. The most significantly regulated pathways in HLCs derived with P2 were the biosynthesis of steroids, which takes place within the liver, and the fetal liver and appendix expression signatures. On the other hand, HLCs obtained with P1 were enriched with genes associated with pancreas and adrenal cortex.

Gene expression signature of HLCs

Transcriptome analysis is a potent tool for deciphering the molecular phenotype and developmental status of hESC- and iPSC-derived cell types. Comparing the gene expression pattern of somatic cells generated in tissue culture with their counterparts in developing organs also interlinks in vitro and in vivo differentiation.

We have compared the transcriptomes of in vitro derived HLCs with those of fetal liver being aware of the fact that fetal liver contains a mixture of cell types and the in vitro culture is enriched in cells possessing hepatocyte-like characteristic. In spite of these differences, we found many common genes and pathways crucial for liver physiology.

A further comparison of the transcriptomes of HLCs, fetal liver, and HLPs revealed that HLCs derived from hESCs and iPSCs have more transcripts in common with fetal liver than with adult liver progenitors, implying that the generated cells show fewer traits in common with adult cells. HLCs and

HLPs share the expression of genes, like *ANXA3* and *EpCAM*, described by us [19] and others [31] as specific for hepatic progenitors. These findings further suggest that stem cell-derived HLCs may contain immature and progenitor-like cells rather than mature hepatocytes. Future studies are warranted to address this problem and aim at generating cells exhibiting a more mature phenotype.

Cytochromes P450 and metabolism of xenobiotics

HLCs should express enzymes crucial for orchestrating drug metabolism and detoxification of which the cytochrome P450 family play a pivotal role. In this regard, we analyzed the expression of cytochromes in HLCs derived from ES and fetal foreskin-derived iPSCs.

Although the HLCs described here exhibit some characteristics of hepatocytes (genes expression/protein profile and hepatic functions), they also appeared to retain some immature characteristics, such as relatively low level expression of cytochrome P450 transcripts and the persistent expression of α -fetoprotein, a marker of fetal rather than adult hepatocytes (Fig. 4).

The expression of 2 key cytochromes *CYP3A4* and *CYP3A7* did not appear to be highly induced in hESCs- and iPSCs-HLCs. Nonetheless, other cytochrome-related enzymes such as *CYP46A1* and *CYP26B1* were significantly upregulated in HLCs compare to undifferentiated cells. Various P450 enzymes are involved in the biosynthesis of low-molecular-weight compounds acting as regulators at various levels and in different processes in human, such as steroids, prostaglandins, thromboxanes, fatty acid derivatives, and derivatives of retinoic acid [32]. The functions of some of these enzymes are not associated with drug metabolism; for example, *CYP11A1* is involved in the first step in the biotransformation of cholesterol, but other P450 enzymes (*CYP1A1*, *CYP1B1*, and *CYP2E1*) that metabolize xenobiotics and drugs known to be expressed in liver were significantly expressed in the HLCs.

Overall, since the high level of drug-metabolizing enzymes is one of the prerequisites for hESC- and iPSC-derived

TABLE 5. LIST OF GENES INVOLVED IN SUBSEQUENT PHASES OF DRUGS METABOLISM

<i>Gene name</i>	<i>hESCs-HLCs_P1</i>	<i>hESCs-HLCs_P2</i>	<i>iPSCs-HLCs_P1</i>
<i>Drug transporters</i>			
MT3	4.369	35.930	4.372
ABCC1	2.528	1.694	2.105
ABCB1	0.765	0.140	0.196
MT2A	0.341	0.024	0.008
<i>Phase I metabolizing enzymes</i>			
CYP2C19	17.725	9.576	13.292
CYP1A1	107.556	1.546	3.256
CYP11B2	6.192	3.967	4.610
CYP2E1	6.969	0.643	3.019
CYP2C9	2.161	0.799	1.169
CYP2F1	2.221	1.413	1.705
CYP2D6	0.158	0.105	0.126
CYP2C8	0.758	0.222	0.358
CYP19A1	0.136	0.036	0.050
CYP3A5	0.019	0.004	0.007
CYP2J2	0.051	0.008	0.009
<i>Phase II metabolizing enzymes</i>			
<i>Carboxylesterases</i>			
CES4	1.941	0.802	0.982
CES2	0.973	0.875	0.628
<i>Decarboxylases</i>			
GAD1	2.257	2.286	1.720
<i>Dehydrogenases</i>			
HSD17B1	3.269	0.391	0.787
HSD17B3	1.265	0.596	0.756
HSD17B2	0.061	0.002	0.003
ADH5	0.580	0.562	0.394
ADH1C	0.569	0.393	0.636
ALDH1A1	0.186	0.004	0.015
ALAD	0.101	0.040	0.043
ADH6	0.012	0.008	0.008
ADH4	0.012	0.004	0.007
<i>Glutathione peroxidases</i>			
GPX2	9.136	0.105	0.164
GPX4	0.906	0.438	0.303
GPX1	0.630	0.207	0.299
GSTZ1	0.525	0.236	0.381
GPX3	0.340	0.029	0.027
MPO	0.003	0.003	0.004
<i>Lipoxygenases</i>			
ALOX15	2.592	1.326	2.057
ALOX5	0.860	0.133	0.178
APOE	0.223	0.016	0.017
ALOX12	0.086	0.055	0.093
<i>Hydrolases</i>			
FAAH	0.463	0.540	0.246
EPHX1	0.060	0.029	0.036
FBP1	0.018	0.004	0.005

(continued)

TABLE 5. (CONTINUED)

<i>Gene name</i>	<i>hESCs-HLCs_P1</i>	<i>hESCs-HLCs_P2</i>	<i>iPSCs-HLCs_P1</i>
<i>Kinases</i>			
<i>PKM2</i>	8.072	4.199	4.310
<i>HK2</i>	5.756	3.470	2.029
<i>PKLR</i>	0.058	0.039	0.047
<i>Oxidoreductases</i>			
<i>NQO1</i>	12.000	3.411	6.101
<i>GPX2</i>	9.136	0.105	0.164
<i>SRD5A2</i>	4.050	3.333	3.246
<i>GSR</i>	1.495	0.903	0.723
<i>CYB5R3</i>	0.976	0.409	0.420
<i>NOS3</i>	0.919	0.182	0.163
<i>GPX1</i>	0.630	0.207	0.299
<i>MTHFR</i>	0.423	0.174	0.189
<i>BLVRA</i>	0.374	0.293	0.260
<i>BLVRB</i>	0.093	0.026	0.038
<i>Paraoxonase</i>			
<i>PON2</i>	0.576	0.565	0.278
<i>PON3</i>	0.031	0.002	0.004
<i>PON1</i>	0.022	0.015	0.021
<i>Glutathione S-Transferases</i>			
<i>GSTP1</i>	2.267	0.655	0.482
<i>GSTM3</i>	2.055	0.900	0.410
<i>GSTA3</i>	0.600	0.432	0.460
<i>GSTM2</i>	0.475	0.453	0.151
<i>MGST3</i>	0.368	0.139	0.072
<i>GSTM5</i>	0.362	0.298	0.306
<i>GSTA4</i>	0.330	0.793	0.691
<i>MGST2</i>	0.303	0.038	0.031
<i>GSTT1</i>	0.169	0.078	0.085
<i>Sulfotransferases</i>			
<i>SULT1A3</i>	0.585	0.286	0.348
<i>SULT1A2</i>	0.329	0.087	0.117
<i>SULT1A1</i>	0.264	0.103	0.170
<i>SULT2A1</i>	0.036	0.009	0.010
<i>UDP-glucuronotransferases</i>			
<i>UGT1A3</i>	20.587	10.658	15.356
<i>UGT1A1</i>	6.514	1.434	2.210
<i>UGT2B4</i>	0.070	0.048	0.075
<i>Transferases</i>			
<i>NAT2</i>	16.176	6.506	9.354
<i>COMT</i>	0.909	0.026	0.502
<i>NAT1</i>	0.845	0.297	0.391
<i>GGT1</i>	0.176	0.037	0.055
<i>Other related genes</i>			
<i>ASNA1</i>	11.991	10.105	10.916
<i>AHR</i>	2.268	1.707	0.966
<i>SNN</i>	1.986	4.287	2.158
<i>MARCKS</i>	1.089	1.548	0.695
<i>ARNT</i>	1.047	0.687	0.645
<i>SMARCAL1</i>	0.646	0.557	0.343

Presented are ratios of expression between HLCs derived with hESCs (hESCs-HLC_P1 and hESCs-HLCs_P2), iPSCs (iPSCs-HLCs_P1), and fetal liver. The ratios marked in gray are above 1 and indicate expression at a level comparable to fetal liver.

hepatocytes to be useful for the investigation of drug metabolism and toxicology, it appears necessary to further improve the differentiation procedures.

Significantly upregulated transcription factors in HLCs might function as drivers for direct transdifferentiation

The differentiation protocols are laborious and it takes around 3 weeks to differentiate pluripotent cells into cells possessing hepatocyte-like features. Recently, it has been shown that mouse fibroblasts can be directly converted into functional neurons, bypassing the intermediate iPSC step [35]. This was obtained by using a combination of transcription factors known to play a critical role in neuronal development. With this approach in mind, our dataset may provide the opportunity to identify transcription factors upregulated in both hESC- and iPSC-derived HLCs.

In particular, we identified 9 transcription factors in common between all HLCs and fetal liver (Table 4). It is tempting to speculate that these factors may represent promising candidates for the induction of functional hepatocytes directly from somatic cells.

In conclusion, our results suggest that an in vitro system for hepatic differentiation is a potent tool for analyzing molecular pathways associated with hepatogenesis. Our analysis also revealed the activation of genes involved in drug metabolism, thus confirming the usefulness of this protocol for the derivation of HLCs for patient-specific drug toxicology screens. However, further effort is warranted to obtain more mature cells and we anticipate that knowledge gained from our study might aid in attaining this ultimate goal.

Acknowledgments

This work was supported in part by BMBF grants (01GN0530, 01GN0807, and 0315398G) and the Max Planck Society.

Author Disclosure Statement

No competing financial interests exist.

References

1. Laconi S, S Montisci, S Doratiotto, M Greco, D Pasciu, S Pillai, P Pani and E Laconi. (2006). Liver repopulation by transplanted hepatocytes and risk of hepatocellular carcinoma. *Transplantation* 82:1319–1323.
2. Cai J, Y Zhao, Y Liu, F Ye, Z Song, H Qin, S Meng, Y Chen, R Zhou, X Song, Y Guo, M Ding and H Deng. (2007). Directed differentiation of human embryonic stem cells into functional hepatic cells. *Hepatology* 45:1229–1239.
3. Agarwal S, KL Holton and R Lanza. (2008). Efficient differentiation of functional hepatocytes from human embryonic stem cells. *Stem Cells* 26:1117–1127.
4. Hay DC, J Fletcher, C Payne, JD Terrace, RC Gallagher, J Snoeys, JR Black, E Wojtacha, K Samuel, Z Hannoun, A Pryde, C Filippi, IS Currie, SJ Forbes, JA Ross, PN Newsome and JP Iredale. (2008). Highly efficient differentiation of hESCs to functional hepatic endoderm requires ActivinA and Wnt3a signaling. *Proc Natl Acad Sci U S A* 105:12301–12306.
5. Hay DC, D Zhao, J Fletcher, ZA Hewitt, D McLean, A Urruticoechea-Uriguen, JR Black, C Elcombe, JA Ross, R Wolf and W Cui. (2008). Efficient differentiation of hepatocytes from human embryonic stem cells exhibiting markers recapitulating liver development in vivo. *Stem Cells* 26:894–902.
6. Song Z, J Cai, Y Liu, D Zhao, J Yong, S Duo, X Song, Y Guo, Y Zhao, H Qin, X Yin, C Wu, J Che, S Lu, M Ding and H Deng. (2009). Efficient generation of hepatocyte-like cells from human induced pluripotent stem cells. *Cell Res* 19:1233–1242.
7. Sullivan GJ, DC Hay, IH Park, J Fletcher, Z Hannoun, CM Payne, D Dalgetty, JR Black, JA Ross, K Samuel, G Wang, GQ Daley, JH Lee, GM Church, SJ Forbes, JP Iredale and I Wilmot. (2010). Generation of functional human hepatic endoderm from human induced pluripotent stem cells. *Hepatology* 51:329–335.
8. Touboul T, NR Hannan, S Corbineau, A Martinez, C Martinet, S Branchereau, S Mainot, H Strick-Marchand, R Pedersen, J Di Santo, A Weber and L Vallier. (2010). Generation of functional hepatocytes from human embryonic stem cells under chemically defined conditions that recapitulate liver development. *Hepatology* 51:1754–1765.
9. Si-Tayeb K, FK Noto, M Nagaoka, J Li, MA Battle, C Duris, PE North, S Dalton and SA Duncan. (2010). Highly efficient generation of human hepatocyte-like cells from induced pluripotent stem cells. *Hepatology* 51:297–305.
10. Takahashi K, K Tanabe, M Ohnuki, M Narita, T Ichisaka, K Tomoda and S Yamanaka. (2007). Induction of pluripotent stem cells from adult human fibroblasts by defined factors. *Cell* 131:861–872.
11. Yu J, MA Vodyanik, K Smuga-Otto, J Antosiewicz-Bourget, JL Frane, S Tian, J Nie, GA Jonsdottir, V Ruotti, R Stewart, Slukvin, II and JA Thomson. (2007). Induced pluripotent stem cell lines derived from human somatic cells. *Science* 318:1917–1920.
12. Singh AM and S Dalton. (2009). The cell cycle and Myc intersect with mechanisms that regulate pluripotency and reprogramming. *Cell Stem Cell* 5:141–149.
13. Park IH, R Zhao, JA West, A Yabuuchi, H Huo, TA Ince, PH Lerou, MW Lensch and GQ Daley. (2008). Reprogramming of human somatic cells to pluripotency with defined factors. *Nature* 451:141–146.
14. Yamanaka S. (2009). A fresh look at iPS cells. *Cell* 137:13–17.
15. Nishikawa S, RA Goldstein and CR Nierras. (2008). The promise of human induced pluripotent stem cells for research and therapy. *Nat Rev Mol Cell Biol* 9:725–729.
16. Asgari S, B Pournasr, GH Salekdeh, A Ghodsizadeh, M Ott and H Baharvand. (2010). Induced pluripotent stem cells: a new era for hepatology. *J Hepatol* 53:738–751.
17. Chin MH, MJ Mason, W Xie, S Volinia, M Singer, C Peterson, G Ambartsumyan, O Aimiwu, L Richter, J Zhang, I Khvorostov, V Ott, M Grunstein, N Lavon, N Benvenisty, CM Croce, AT Clark, T Baxter, AD Pyle, MA Teitell, M Pelegri, K Plath and WE Lowry. (2009). Induced pluripotent stem cells and embryonic stem cells are distinguished by gene expression signatures. *Cell Stem Cell* 5:111–123.
18. Feng Q, SJ Lu, I Klimanskaya, I Gomes, D Kim, Y Chung, GR Honig, KS Kim and R Lanza. (2010). Hemangioblastic derivatives from human induced pluripotent stem cells exhibit limited expansion and early senescence. *Stem Cells* 28:704–712.
19. Xu C, MS Inokuma, J Denham, K Golds, P Kundu, JD Gold and MK Carpenter. (2001). Feeder-free growth of undif-

- ferentiated human embryonic stem cells. *Nat Biotechnol* 19:971–974.
20. Prigione A, B Fauler, R Lurz, H Lehrach and J Adjaye. (2010). The senescence-related mitochondrial/oxidative stress pathway is repressed in human induced pluripotent stem cells. *Stem Cells* 28:721–733.
 21. Jozefczuk J, H Stachelscheid, L Chavez, R Herwig, H Lehrach, K Zeilinger, JC Gerlach and J Adjaye. (2010). Molecular characterization of cultured adult human liver progenitor cells. *Tissue Eng Part C Methods* 16:821–834.
 22. Branch RA. (1982). Drugs as indicators of hepatic function. *Hepatology* 2:97–105.
 23. Hay DC, D Zhao, A Ross, R Mandalam, J Lebkowski and W Cui. (2007). Direct differentiation of human embryonic stem cells to hepatocyte-like cells exhibiting functional activities. *Cloning Stem Cells* 9:51–62.
 24. Gentleman RC, VJ Carey, DM Bates, B Bolstad, M Dettling, S Dudoit, B Ellis, L Gautier, Y Ge, J Gentry, K Hornik, T Hothorn, W Huber, S Iacus, R Irizarry, F Leisch, C Li, M Maechler, AJ Rossini, G Sawitzki, C Smith, G Smyth, L Tierney, JY Yang and J Zhang. (2004). Bioconductor: open software development for computational biology and bioinformatics. *Genome Biol* 5:R80.
 25. Dunning MJ, ML Smith, ME Ritchie and S Tavare. (2007). beadarray: R classes and methods for Illumina bead-based data. *Bioinformatics* 23:2183–2184.
 26. Team RDC. (2009). R: A language and environment for statistical computing. R Foundation for Statistical Computing. www.r-project.org/
 27. Saeed AI, V Sharov, J White, J Li, W Liang, N Bhagabati, J Braisted, M Klapa, T Currier, M Thiagarajan, A Sturm, M Snuffin, A Rezantsev, D Popov, A Ryltsov, E Kostukovich, I Borisovsky, Z Liu, A Vinsavich, V Trush and J Quackenbush. (2003). TM4: a free, open-source system for microarray data management and analysis. *Biotechniques* 34:374–378.
 28. Huang da W, BT Sherman and RA Lempicki. (2009). Systematic and integrative analysis of large gene lists using DAVID bioinformatics resources. *Nat Protoc* 4:44–57.
 29. Dennis G, Jr., BT Sherman, DA Hosack, J Yang, W Gao, HC Lane and RA Lempicki. (2003). DAVID: database for annotation, visualization, and integrated discovery. *Genome Biol* 4:P3.
 30. Snel B, G Lehmann, P Bork and MA Huynen. (2000). STRING: a web-server to retrieve and display the repeatedly occurring neighbourhood of a gene. *Nucleic Acids Res* 28:3442–3444.
 31. Schmelzer E, E Wauthier and LM Reid. (2006). The phenotypes of pluripotent human hepatic progenitors. *Stem Cells* 24:1852–1858.
 32. Hines RN and DG McCarver. (2002). The ontogeny of human drug-metabolizing enzymes: phase I oxidative enzymes. *J Pharmacol Exp Ther* 300:355–360.
 33. Ge X, S Yamamoto, S Tsutsumi, Y Midorikawa, S Ihara, SM Wang and H Aburatani. (2005). Interpreting expression profiles of cancers by genome-wide survey of breadth of expression in normal tissues. *Genomics* 86:127–141.
 34. Heutinck KM, IJ ten Berge, CE Hack, J Hamann and AT Rowshani. (2010). Serine proteases of the human immune system in health and disease. *Mol Immunol* 47:1943–1955.
 35. Vierbuchen T, A Ostermeier, ZP Pang, Y Kokubu, TC Sudhof and M Wernig. (2010). Direct conversion of fibroblasts to functional neurons by defined factors. *Nature* 463:1035–1041.

Address correspondence to:

Dr. James Adjaye
Max Planck Institute for Molecular Genetics
Department of Vertebrate Genomics
Molecular Embryology and Aging group
Ilhnestrasse 73, D-14195
Berlin
Germany

E-mail: adjaye@molgen.mpg.de

Received for publication August 24, 2010

Accepted after revision December 16, 2010

Prepublished on Liebert Instant Online Month 00, 0000

